PAPER • **OPEN ACCESS**

Influence of aluminium alloys relative positioning on dissimilar friction stir lap welds properties

To cite this article: S Sabari *et al* 2020 *IOP Conf. Ser.: Mater. Sci. Eng.* **968** 012018

IOP Conf. Series: Materials Science and Engineering **968** (2020) 012018 doi:10.1088/1757-899X/968/1/012018

Influence of aluminium alloys relative positioning on dissimilar friction stir lap welds properties

S Sabari[1], I Galvão[1,2], C Leitão[1] and D M Rodrigues[3]
[1] CEMMPRE, Department of Mechanical Engineering, University of Coimbra, Portugal
[2] ISEL, Department of Mechanical Engineering, Polytechnic Institute of Lisbon, Portugal
[3] ISISE, Department of Mechanical Engineering, University of Coimbra, Portugal

E-mail: sree.sabari@dem.uc.pt

Abstract. Very thin sheets of heat treatable (AA6082-T6) and non-heat treatable (AA5754-H22) aluminium alloys were used to produce dissimilar joints by friction stir lap welding. Joint strength and mechanical heterogeneity were assessed by performing lap tensile-shear and microhardness testing, respectively. Optical microscopy was used to analyse the weld morphology. Welding machine outputs, such as torque and axial force, were analysed in order to capture differences in the alloys strength during dissimilar welding. From the process outputs analysis, it was concluded that higher Z-Forces were necessary while positioning the AA5754 alloy at the top of lap configuration, indicating that this alloy offered higher resistance to the tool stirring than the AA6082 alloy. These results were associated with the flow softening of the AA6082 alloy during welding, which was explained using finite element analysis to illustrate the welding thermal cycles and the precipitation behaviour of this alloy. The lap welds defect formation was also related to the base materials plastic properties at high temperatures, which was inferred from process outputs data analysis. Based on the results it was shown that the lap welds defects might be supressed by a proper positioning the dissimilar base materials in the lap joint.

1. Introduction

Friction stir welding (FSW) is a prominent technique that is already used for the successful joining of similar aluminium materials. However, compared to similar welding, dissimilar FSW is still a challenge since the interaction of base materials with different properties is required [1]. Simar et al., 2010, for example, welded AA2017 to AA6005A and found a similar kind of precipitate-related softening during welding, since both alloys are heat treatable [2]. However, when welding heat treatable and non-heat treatable aluminium alloys, the exposure of the dissimilar materials to high temperatures may leads to different microstructure-related softening responses [3]. It is widely known that recovery is the primary softening mechanism in non-heat treatable aluminium alloys, whereas precipitate dissolution or coarsening are the primary softening mechanism in heat treatable alloys [4, 5]. Considering the differences in the softening mechanisms between the heat treatable and non-heat treatable alloys, differences in flow behaviour during welding may be also expected.

The dissimilar flow behaviour of the base materials may have important influence on weld morphology, especially for lap joint configuration, where the upward material flow results in hook and cold lap defects formation [6]. Cederqvist & Reynolds, 2001 reported that the hook defect reduces the effective joining thickness [7] and Chen, 2012 referred that increments in hook height reduce the joint strength [8]. Many researchers, including Cao & Jahazi, 2011 [9] and Yazdanian et al., 2012 [10], adapted the process parameters and tool profiles for regulating the material flow in order to suppress the hook defect. But, from the studies made by Leitão, 2013 [11] and Galvão et al., 2013 [12] it was inferred that the inherent base material plastic properties are the key factor deciding the material flowability. Considering this aspect, Costa et al., 2015 explored the idea of changing the position of the aluminium alloys in the lap configuration to control the upward material flow and thereby to control the hook formation [13].

However, although the influence of the base materials positioning on weld properties was already addressed in a large number of works on dissimilar butt joining, the analysis of base materials positioning on lap welds quality, especially for the joining of very thin sheets, is scarce. Moreover, the relationship between the morphological and the mechanical properties of lap welds and the softening mechanisms of the base materials is not defined yet. This way, the aim of the present work was to analyse the influence of the relative positioning of the base materials on the properties of very thin AA6082/AA5754 friction stir lap welds. The softening mechanisms and their influence on the material flow were especially addressed. A coupled experimental and numerical approach was followed in this study.

2. Experimental procedure

One mm-thick sheets of the heat treatable AA6082-T6 and the non-heat treatable AA5754-H22 aluminium alloys were used as base materials to produce dissimilar friction stir lap welds. The alternative positioning of the base materials in the lap joint was tested, i.e. while some welds were produced with the AA6082 alloy positioned in the top of the joint, other welds were produced with the reverse positioning of the materials. In the text, the dissimilar welds made by placing the AA5754 alloy in the top of the joint will be labelled as D56, whereas the dissimilar welds made with the reverse base materials positioning will be designated as D65. In order to better understand the role of the dissimilar base materials flow on welds properties, three tools with different pin profiles and dimensions were used. Details on the used pin profiles, which were labelled according to their design (cylindrical - CL; conical - CN) and diameter, are displayed in Table 1. Following Costa et al., 2018, the tool rotational and traverse speeds were set equal to 600 rpm and 300 mm/min, respectively, the tool tilt angle was 2° and the tool plunge depth was 1.2 mm (positioning control). During the welding trials, the torque and force evolution was recorded [14].

Table 1. Geometries and dimensions of the pin profiles.

Tool designation	Cylindrical-CL6	Conical-CN6	Conical-CN8
Dimensions [mm]	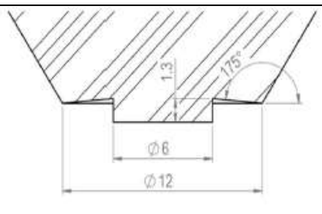	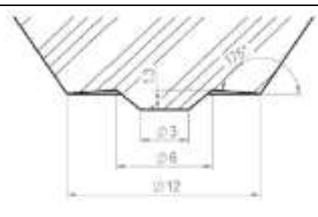	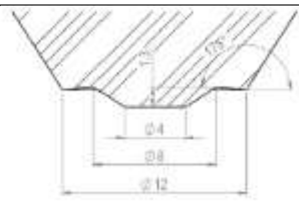

The cross-section of the welds was analysed in order to characterise the weld morphology. Keller's etchant was used to differentiate the flow of the different base materials. The mechanical properties of the dissimilar welds were evaluated by performing lap tensile-shear tests and microhardness measurements. The tensile-shear specimens were collected transversely to the welding direction. Advancing (AS) and retreating (RS) side loading schemes, defined based on Costa et al., 2018, were tested to assess the lap weld strength asymmetry [14].

3. Numerical simulation details

A thermal analysis of the lap welding process was done using finite element (FE) numerical simulation in order to correlate the temperature distribution in the similar joints with the precipitation behaviour of the AA6082 alloy. A simple FE FSW modelling approach was handled herewith by considering the AA6082 alloy as the only base material since the softening at the heat treatable alloy was the main phenomena of interest. FE modelling was done according to the procedures reported by Dialami et al., 2017 [15] and Andrade et al., 2020 [16]. The AA6082 alloy precipitation kinetics under the thermal conditions developed during welding was found using Thermocalc metallurgical software and correlated with the FE results.

4. Results and discussion

4.1. Mechanical properties

In order to understand the weld performance, tensile-shear testing was conducted by loading AS and RS specimens. The peak load values of the welds and the base materials are shown in Figure 1. From the figure it can be observed that all the welds were in under match when compared to both base materials. However, the D65 welds displayed higher load values than the D56 welds, which is especially noticed for the AS-loaded specimens. It can also be observed that the asymmetry in strength between the AS and the RS-loaded specimens is more evident for the D56 welds than for D65 welds. The RS-tested D56 specimens presented higher load values than the AS-tested specimens for all the used tools. On the other hand, the D65 weld produced with the CN8 tool performed well in both AS and RS loading conditions.

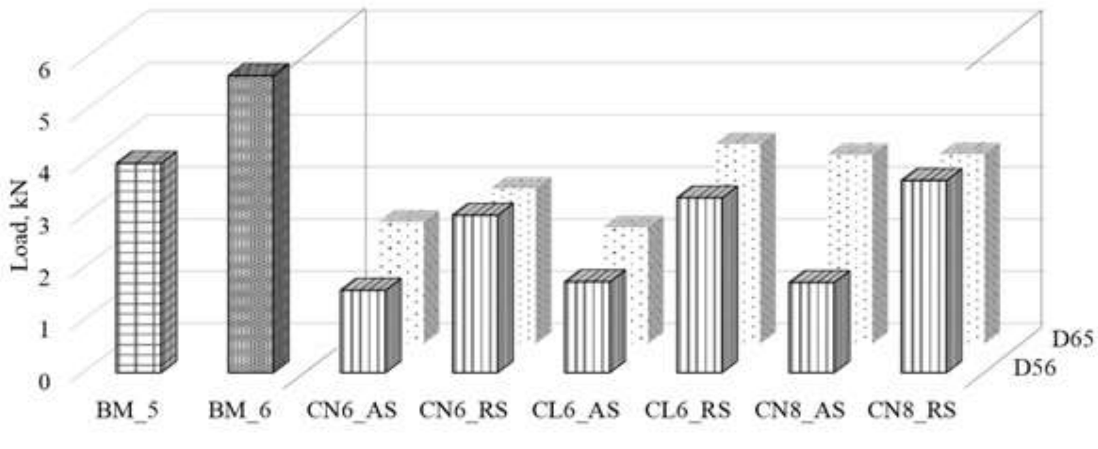

Figure 1. Tensile-shear properties of the welds and the base materials.

4.2. Force and torque analysis

Figure 2 displays the average values of Torque (Figure 2a) and Z-Force (Figure 2b) registered during welding. These values were computed considering only the steady-state stage of the process, i.e. discarding the initial and final instabilities. From Figure 2a, it can be observed that no important differences exist in the Torque values registered for the welds produced with different tools. As the part of the tool that drags most material during welding is the shoulder, which was similar for all the tools, it is easy to understand the non-variation in Torque among the different weld series.

Figure 2b shows that the Z-Force values varied according to both the tool and the base material positioning. Regarding the influence of the tool, lower Z-Force values were registered for the welds produced with the CN8 tool. This observation is agreeing with the previous study reported by Costa et al., 2015, where, axial force increases linearly with increasing shoulder plunge depth of different pin profiles [13]. So, with reference to that, it can say that the lower Z-Force of CN8 tool is attributed to the lower shoulder plunge depth. In which concerns to the positioning of the base materials, it can be observed that the D65 welds required lower Z-Force values than the D56 welds. Arora et al., 2011 related the evolution of the Z-Force with the material properties and reported the higher flow strength of the material as the reason for recording higher Z-Force values [17]. According to Leitão et al., 2012, the 5XXX aluminium alloys present higher flow strength at high temperature and strain rates than the 6XXX alloys [11]. Since the AA6082 is the most dragged material in the D65 welds, the lower Z-Force values agree-well with the mechanical behaviour of this alloy.

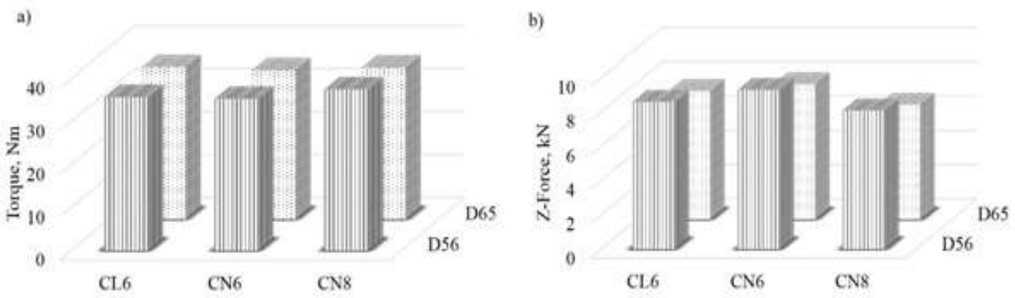

Figure 2. FSW machine process outputs: a) Torque; b) Z-Force.

4.3. Morphological characterisation

It is important to understand the influence of the flow strength and the positioning of the alloys on the material flow during welding. Figure 3 illustrates macrographs of the transverse cross-sections of the D65 (Figure 3a) and D56 (Figure 3b) welds produced with the CN8 tool. From Figure 3a, it can be observed that the cross-section of the D65 welds is free of defects. In turn, Figure 3b shows that hook formation occurred in the AS of the D56 welds. This agrees-well with the very low strength presented by these joints during AS loading, and therefore, with the strong asymmetry in strength between the AS and the RS. On the other hand, the smaller asymmetry in strength observed for the D65 welds is explained by the non-formation of defects.

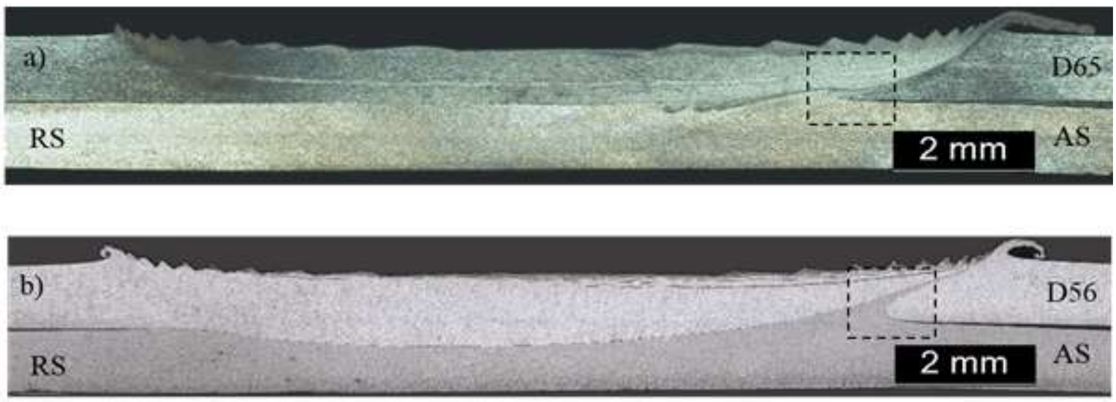

Figure 3. Macrostructure of the weld cross-sections: a) D65-CN8 weld; b) D56-CN8 weld.

Liu et al., 2016 explained that hook forms due to the upward material flow occurring at the AS [18]. Therefore, the lower hook height of the D65 welds clearly indicates that the placement of AA5754 plate at the bottom of the joint hinders the upward material flow. On the other hand, when the AA6082 alloy, which presents lower flow strength, is located at the bottom, the upward material flow is intense and hook formation is facilitated. The orientation of the hook along the thickness direction reduces the effective thickness of the top plate, and consequently, the load bearing area of the D56 AS-tested specimens.

4.4. Influence of base materials

In order to understand the differences in material flow between both dissimilar welds, the base materials softening mechanisms during welding should be understood. Figure 4a shows the hardness distribution along the longitudinal section of the top plate of the CN8 dissimilar welds. The central region of the graph, in which no microhardness values are displayed, corresponds to the pin zone, whereas the left and the right regions correspond to the trailing and the leading sides of the tool, respectively. From the figure, it can be observed that the microhardness values of the AA6082 alloy are under matched relative to the base material at both the trailing and the leading (pre-heat zone) sides of the tool. On the other hand, the microhardness of the AA5754 alloy is similar to that of the base material, or even higher, in some localised zones. These results agree-well with the previously-reported softening tendency of the AA6082 alloy with the temperature. Unlike the AA5754 alloy, the AA6082 alloy gets well softened before entering the processing zone, which may be one of the reasons for its higher flowability. So, placing the softer AA6082 at the bottom of the joint promotes the upward material flow, leading to a high hook height (Figure 3b), and consequently, affecting the strength of the welds (Figure 1).

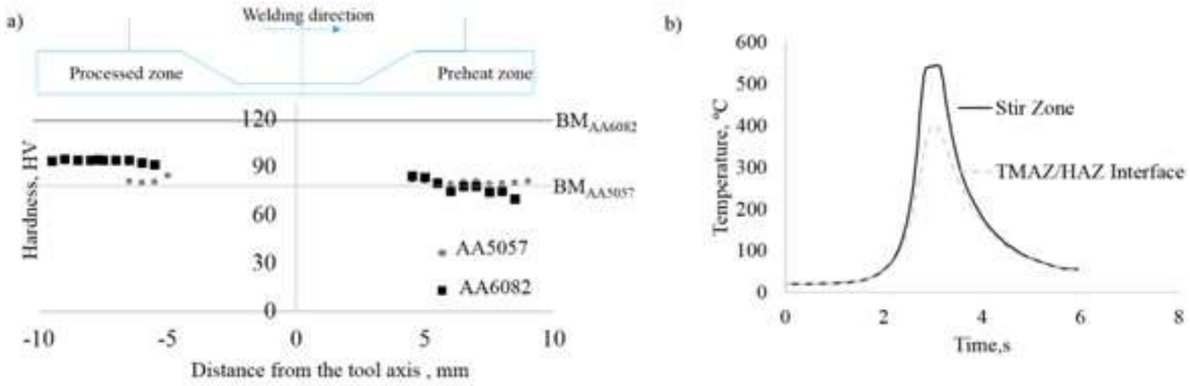

Figure 4. Thermomechanical characterisation: a) Microhardness profile along the welding direction; b) Thermal cycles obtained by FE simulation.

Table 2. Simulated dissolution temperatures of the precipitates.

Precipitate	GP Zone	β”	β’	β
Dissolution Temperature, °C	133 °C	325 °C	468 °C	530 °C

As illustrated in Figure 4b, where are shown the thermal cycles obtained by FE simulation, the peak temperatures in the stir zone and TMAZ/HAZ interface were of 553 °C and 400 °C, respectively. To get more insight about the softening mechanism of the AA6082 alloy, the possible precipitate evolutions and their respective dissolution temperatures were simulated and are displayed in Table 2. By correlating the thermal cycles and the precipitate dissolution temperatures, it is understood that the processed zone undergoes β dissolution whereas the temperature attained in the preheat zone or HAZ/TMAZ interface is not sufficient for β’ dissolution and thereby it is assumed that β’ coarsening may be occurred and yet it undergone β” dissolution. The precipitate dissolution/coarsening is exactly agreeing with the lower hardness regions of AA6082 alloy.

IOP Conf. Series: Materials Science and Engineering **968** (2020) 012018 doi:10.1088/1757-899X/968/1/012018

5. Conclusions

A coupled experimental and numerical research was developed to analyse the influence of the relative positioning of the base materials on the properties of very thin AA6082/AA5754 friction stir lap welds. From this research, the following conclusions can be drawn:

- The heat treatable AA6082 aluminium alloy exhibits lower flow strength and higher dynamic softening effect than the non-heat treatable AA5754 aluminium alloy during welding.
- The softening of the AA6082 aluminium alloy promotes upward material flow when this alloy is located at the bottom of the joint, which results in hook defect formation, and consequently, in the deterioration of the tensile-shear properties of the welds.
- Welds with a good mechanical behaviour can be achieved by positioning the AA5754 aluminium as the bottom plate in the joint. The higher flow strength and lower softening of the AA5754 alloy supress hook formation in these welds.

6. References

[1] Leitao C, Leal R M, Rodrigues D M, Loureiro A and Vilaça P 2009 *Mater. Des.* **30** 101–8
[2] Simar A, Jonckheere C, Deplus K, Pardoen T and De Meester B 2010 *Sci. Technol. Weld. Join.* **15** 254–9
[3] Jamshidi Aval H, Serajzadeh S and Kokabi A H 2011 *Mater. Sci. Eng. A* **528** 8071–83
[4] Wu L and Ferguson W G 2009 *Mater. Sci. Forum* **618–619** 203–6
[5] Summers P T, Chen Y, Rippe C M, Allen B, Mouritz A P, Case S W and Lattimer B Y 2015 *Fire Sci. Rev.* **4** 3
[6] Costa M I, Leitão C and Rodrigues D M 2017 *J. Mater. Process. Technol.* **250** 289–96
[7] Cederqvist L and Reynolds A P 2001 *Weld. J. (Miami, Fla)* **80** 281–287
[8] Z.W. Chen S Y 2012 *J. Achiev. Mater. Manuf. Eng.* **55** 629–37
[9] Cao X and Jahazi M 2011 *Mater. Des.* **32** 1–11
[10] Yazdanian S, Chen Z W and Littlefair G 2012 *J. Mater. Sci.* **47** 1251–61
[11] Leitão; C 2013 *Influence of Base Material Plastic Properties and Process Parameters on Friction Stir Weldability* (University of Coimbra, Portugal)
[12] Galvão I, Verdera D, Gesto D, Loureiro A and Rodrigues D M 2013 *J. Mater. Process. Technol.* **213** 1920–8
[13] Costa M I, Verdera D, Leitão C and Rodrigues D M 2015 *Mater. Des.* **87** 721–31
[14] Costa M I, Leitao C and Rodrigues D M 2018 *Soldag. Inspeção* **23** 32–42
[15] Dialami N, Cervera M, Chiumenti M and Agelet de Saracibar C 2017 *Int. J. Mech. Sci.* **122** 215–27
[16] Andrade D G, Leitão C, Dialami N, Chiumenti M and Rodrigues D M 2020 *Int. J. Mech. Sci.* **182** 105725
[17] Arora A, De A and DebRoy T 2011 *Scr. Mater.* **64** 9–12
[18] Liu H, Hu Y, Peng Y, Dou C and Wang Z 2016 *J. Mater. Process. Technol.* **238** 244–54

Acknowledgements

This research is sponsored by FEDER funds through Portugal 2020 (PT2020), by the Competitiveness and Internationalization Operational Program (COMPETE 2020) and national funds through the Portuguese Foundation for Science and Technology, under the projects: UID/EMS/00285/2020, POCI-01-0145-FEDER-00763 and Friction 4.0(POCI-01-0145-FEDER-032089). All supports are gratefully acknowledged.